Vapor–Solid Growth of High Optical Quality MoS_2 Monolayers with Near-Unity Valley Polarization

Sanfeng Wu,[†,§] Chunming Huang,[†,§] Grant Aivazian,[†] Jason S. Ross,[‡] David H. Cobden,[†] and Xiaodong Xu[†,‡,*]

[†]Department of Physics and [‡]Department of Material Science and Engineering, University of Washington, Seattle, Washington 98195, United States. [§]These authors contributed equally to this work.

ABSTRACT Monolayers of transition metal dichalcogenides (TMDCs) are atomically thin direct-gap semiconductors with potential applications in nanoelectronics, optoelectronics, and electrochemical sensing. Recent theoretical and experimental efforts suggest that they are ideal systems for exploiting the valley degrees of freedom of Bloch electrons. For example, Dirac valley polarization has been demonstrated in mechanically exfoliated monolayer MoS_2 samples by polarization-resolved photoluminescence, although polarization has rarely been seen at room temperature. Here we report a new method for synthesizing high optical quality monolayer MoS_2 single crystals up to 25 μm in size on a variety of standard insulating substrates (SiO_2, sapphire, and glass) using a catalyst-free vapor–solid growth mechanism. The technique is simple and reliable, and the optical quality of the crystals is extremely high, as demonstrated by the fact that the valley polarization approaches unity at 30 K and persists at 35% even at room temperature, suggesting a virtual absence of defects. This will allow greatly improved optoelectronic TMDC monolayer devices to be fabricated and studied routinely.

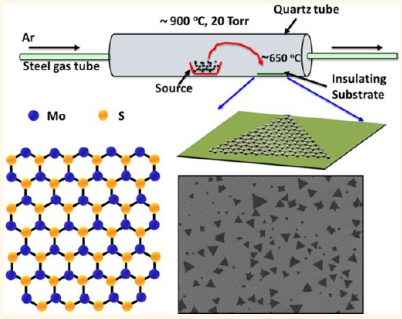

KEYWORDS: molybdenum disulfide · monolayer · vapor–solid growth · photoluminescence · valley polarization · valleytronics

Transition metal dichalcogenides MX_2 (M = Mo, W; X = S, Se, *etc.*) have layered structures with van der Waals interactions between the layers. Monolayers of such materials were first obtained by the mechanical exfoliation technique typically used for graphene.[1] Subsequent investigation has shown that these two-dimensional (2D) semiconductors[1−3] exhibit unique properties, such as a transition from an indirect band gap in the bulk to a direct band gap at monolayer thicknesses,[3,4] massive Dirac-like behavior of the electrons,[5] excellent field-effect transistor performance at room temperature,[6] and completely tunable 2D excitonic effects.[7]

Recently, these monolayers have also been suggested as good candidates for the realization of valley-based electronics.[5,8−10] In monolayer MoS_2, there are two energy-degenerate Dirac valleys at the corners of the hexagonal Brillouin zone.[5,10] The Berry curvature and magnetic moments of electrons associated with different valleys have opposite sign and are linked to measurable quantities which can distinguish the valleys, such as k-resolved optical dichroism, offering the possibility of manipulating and utilizing the valley degree of freedom.[11,12] Valley polarization has been demonstrated in MoS_2 monolayers by circularly polarized light excitation,[8−10] and electrical control of it has been reported in bilayer samples.[13]

Progress thus far has relied mainly on mechanically exfoliated samples where scaling for device applications[14] is probably impossible. Recent attempts to develop more scalable techniques include exfoliation in liquids,[2,15,16] hydrothermal synthesis,[17] epitaxy growth using graphene,[18] and soft sulfurization.[19,20] However, these methods are not easily integrated with device fabrication. Chemical vapor deposition has also been explored using a Mo film[21] (or MoO_3 powder[22]) and sulfur powder as the reactants, yielding monolayers of MoS_2 on 300 nm SiO_2/Si substrate compatible with device fabrication.[21,22] It has yet to be proven though that such monolayers have sufficient quality for investigating valley-related physics. Intervalley scattering

* Address correspondence to xuxd@uw.edu.

Received for review January 14, 2013 and accepted February 22, 2013.

Published online February 22, 2013
10.1021/nn4002038

enhanced by defects and impurities can reduce or destroy the valley polarization, as evident from the disparate degrees of polarization reported by different groups.[8−10,13,23] A high degree of valley polarization is required for valley physics and is also a hallmark of crystal quality.

Here we introduce a new and straightforward method for obtaining high optical quality monolayer MoS_2 *via* a vapor−solid (VS) growth mechanism.[24] Up to 400 μm^2 monolayer flakes with triangular shape are directly produced on insulating substrates such as SiO_2, sapphire, and glass, without using any catalysts. The growth procedure is simple physical vapor transport, using a MoS_2 powder source and Ar carrier gas (details are given in Figure 1 and Methods), similar to the procedure used for growing Bi_2Se_3 topological insulator nanoplates.[24] Using polarization-resolved photoluminescence (PL),[13] we observe valley polarization approaching near-unity at low temperature (30 K) and 35% at room temperature. This observation demonstrates that these monolayers are of high quality and are suitable for valley physics and applications.

RESULTS AND DISCUSSION

The resulting MoS_2 monolayers are characterized by optical microscopy (OM, Zeiss Axio Imager A1), atomic force microscopy (AFM, Veeco Dimension 3100), scanning electron microscopy (SEM, FEI Sirion), and micro-Raman spectroscopy (Renishaw inVia Raman Microscope). Figure 2 is a typical SEM image of a sample grown on SiO_2/Si. The crystallites have lateral dimensions up to 25 μm and are approximately equilateral triangles (see Figure 2 inset). This is consistent with the triangular symmetry of monolayer MoS_2 (Figure 1c). It suggests that each is a single crystal without extended defects or grain boundaries;[25,26] the facets are then the most slow-growing or stable symmetry-equivalent crystal planes—it remains to be established whether these are the "zigzag" or the "armchair" edges. Therefore, another advantage over exfoliation techniques is that the crystal axes can be immediately identified by inspection.

Optical and AFM Characterization. Figure 3a−c shows optical microscope images of growth on sapphire, glass, and 300 nm SiO_2/Si substrates, respectively. The color contrast of all of the larger crystallites is uniform; moreover, for those on SiO_2/Si (Figure 3c), it is identical to that of exfoliated monolayers on the same substrate. These facts strongly indicate that they are monolayers.[3,27] The growth on sapphire is much denser than that on both SiO_2 and glass, but on all of the substrates, nucleation appears to be random, as was found for VS growth of topological insulators.[24] Smaller (<2 μm), thicker crystallites are also present, especially on SiO_2. We speculate that the growth kinetics are such that a monolayer is favored and grows rapidly if the nucleating crystal is aligned suitably with the substrate; otherwise, more three-dimensional growth occurs. The

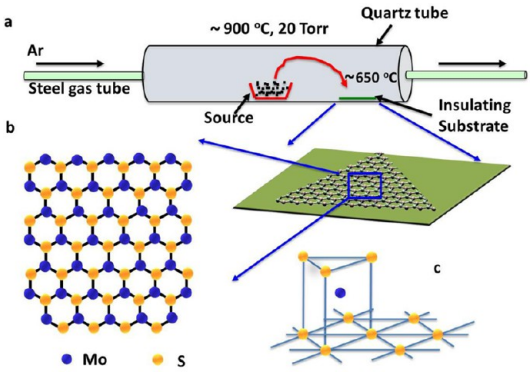

Figure 1. (a) Growth setup and conditions. (b) Cartoon indicating the structure of the triangular monolayer crystallites. (c) Structure of monolayer MoS_2.

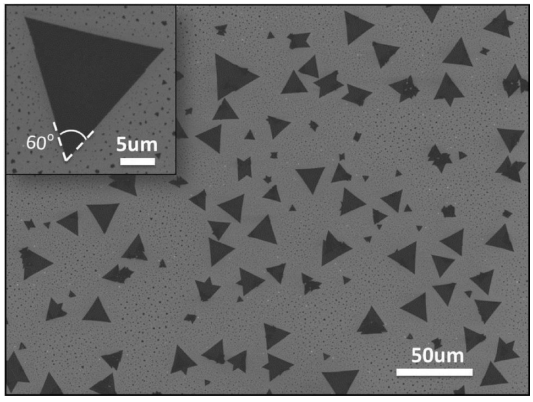

Figure 2. Scanning electron microscope image of triangular MoS_2 monolayer crystallites grown on a 300 nm SiO_2/Si substrate. The inset shows the 60° corners of a selected crystallite with a clean surface.

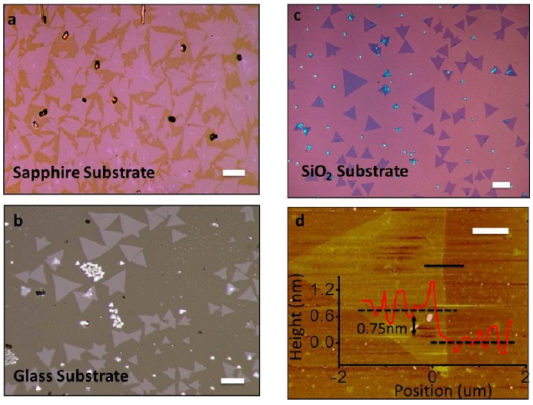

Figure 3. Optical microscope images of MoS_2 crystallites grown on (a) sapphire, (b) glass, and (c) SiO_2/Si. Scale bar is 10 μm. A typical triangular crystallite is further characterized by (d) AFM image with 3 μm scale bar. The inset plot is the height profile along the black line shown in the image, demonstrating its monolayer thickness.

monolayer thickness is confirmed by atomic force microscopy (AFM).[3,6,28] Figure 3d shows an AFM image of one crystallite on SiO_2, revealing a flat, uniform surface. A line cut along the red line (Figure 3e) shows

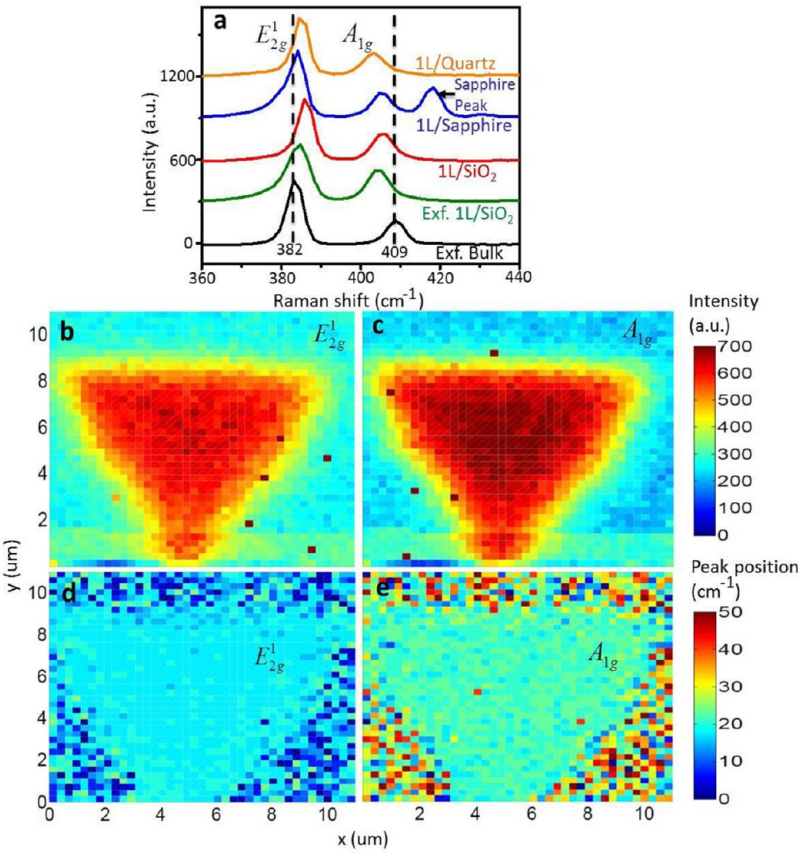

Figure 4. (a) Raman spectra of monolayer MoS_2 grown on different substrates, excited by a 514.5 nm laser. For comparison, the spectra from a mechanically exfoliated monolayer and a bulk MoS_2 crystal are also shown. (b,c) Intensity maps of the two Raman modes, excited by a 532 nm laser line from a typical crystallite. (d,e) Corresponding peak position maps.

an apparent thickness of ~0.75 nm on the SiO_2/Si substrate, consistent with previous measurements of monolayers.[4,6] Similar measurements on sapphire substrates are shown in the Supporting Information.

Raman Characterization. The samples were also studied by Raman spectroscopy. Typical Raman spectra from the triangular crystallites grown on different substrates, as well as from exfoliated monolayer and bulk MoS_2, using a 514.5 nm excitation laser, are shown in Figure 4. We observe both of the Raman modes (E^1_{2g} and A_{1g}) expected for monolayer MoS_2.[3,4,28,29] The E^1_{2g} peak is at 386 cm^{-1} for the SiO_2 substrate, 384 cm^{-1} for sapphire, and 385 cm^{-1} for glass. The A_{1g} peak is at 405 cm^{-1} for SiO_2 and sapphire and 404 cm^{-1} for glass. The peak separations are 19, 21, and 19 cm^{-1}, respectively. All of these numbers agree well with the exfoliated monolayer sample. In order to investigate the uniformity of the grown monolayer sample, we also performed scanning Raman measurements (excited by a 532 nm laser line). Intensity and peak position maps for a triangular crystallite are shown in Figure 4b–e. Note that the different excitation energy leads to a different intensity ratio between the two peaks. The peak separation resulting from the map is 22 ± 1.5 cm^{-1}. It clearly demonstrates that this entire crystallite is a uniform monolayer.

Optical Valley-Selective Effect. To investigate the potential of these monolayer crystallites for 2D optoelectronics and valley-related device applications, we performed polarization-resolved PL.[8,9,13] Circularly polarized PL measurements can identify valley polarization in monolayer MoS_2 created by appropriate optical pumping: the $+K$ and $-K$ valleys are selectively excited by σ^+ or σ^- light, respectively, as indicated Figure 5a.[5,10] Due to the large k-space separation of the valleys, intervalley scattering is suppressed and the valley relaxation time is longer than the electron–hole recombination time. Emission from a given valley is also circularly polarized, and the degree to which the PL has the same helicity as the incident light therefore reflects the degree of valley polarization. Large valley polarization provides evidence for good sample quality, as impurities and defects in the crystal will cause intervalley scattering even at low temperature.[9]

In our measurements, a 632 nm He–Ne laser beam is circularly polarized by a quarter-wave plate (QWP) and focused at normal incidence onto the monolayer sample held in a cryostat. The PL signal is selectively detected for both σ^+ and σ^- polarization using the setup described in ref 13. The laser spot size is about 2 μm with an intensity of ~150 W/cm^2. We define the degree of PL polarization, which reflects the valley

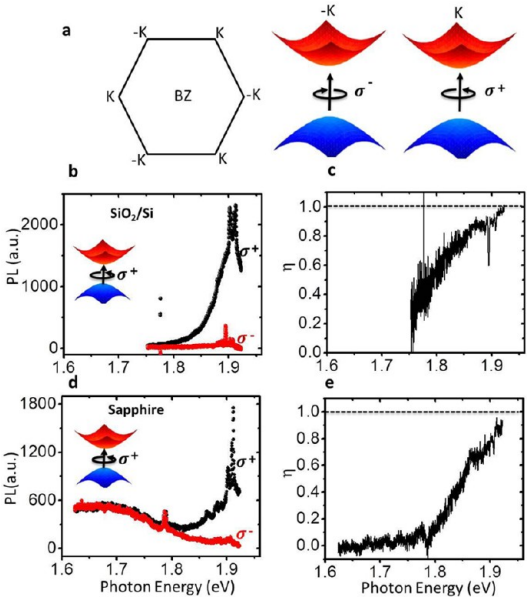

Figure 5. (a) Brillouin zone and K-point band edges in monolayer MoS_2 indicating the optical selection rule. (b) σ^+ (black) and σ^- (red) components of the PL signal for our monolayer MoS_2 on a SiO_2/Si substrate, excited by σ^+ laser light at 632 nm wavelength at 30 K. (c) Degree of PL polarization *vs* photon energy, calculated from (b). (d,e) Corresponding observations on a sample grown on a sapphire substrate. The polarization approaches unity on both substrates.

polarization, as[8,9,13] $\eta = (\mathrm{PL}(\sigma^+) - \mathrm{PL}(\sigma^-))/(\mathrm{PL}(\sigma^+) + \mathrm{PL}(\sigma^-))$.

For a substrate temperature of 30 K, the PL spectra for σ^+ excitation are shown in Figure 5b,d for monolayer crystallites on SiO_2 and sapphire substrates. The results with σ^- excitation are similar (see Supporting Information). The cutoff in the spectra at ~1.92 eV is due to the notch filter placed in the collection optical path for blocking the laser light. The sharp spikes superimposed on the spectra are Raman scattering peaks. The spectra show only a single emission peak at ~1.9 eV in SiO_2 substrate, in contrast with reports on exfoliated samples[30] where a second broad impurity peak is present at ~1.77 eV. The absence of an impurity peak is powerful evidence of excellent crystal quality.[30]

The PL signal is highly σ^+-polarized for both substrates. Reported degrees of valley polarization at low temperatures from mechanically exfoliated monolayers in the literature vary widely: 30,[9] 50,[10] 80,[13] and up to 100% on boron nitride substrate,[8] showing that

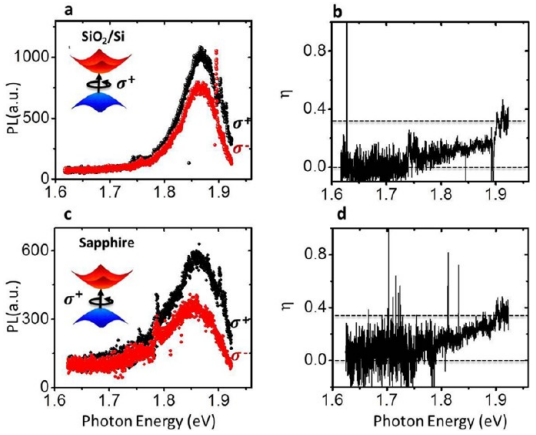

Figure 6. (a) σ^+ and σ^- components of the PL for monolayer on SiO_2/Si substrate, and (b) degree of PL circular polarization *vs* photon energy at room temperature. (c,d) Similar measurements on a sapphire substrate. Up to ~35% polarization is observed on both substrates.

intervalley scattering is very sensitive to sample details. The degree of polarization in our monolayers is plotted in Figure 5c,e for both SiO_2 and sapphire substrates. We see near-unity polarization on SiO_2 and more than 95% on sapphire, with the polarization decreasing at lower photon energies as in previous reports.[8,9]

Interestingly, the PL polarization is substantial even at room temperature, approaching a maximum of 35% at ~1.92 eV on both substrates, as shown in Figure 6. Intervalley scattering increases with temperature due to enhanced phonon populations,[5] resulting in the decrease of the valley polarization and usually making it vanish at room temperature,[9] although recently,[23] there has been a report of 40% of valley polarization at 300 K from a mechanical exfoliation sample. Thus our VS grown samples are as good as the highest optical quality samples obtained by mechanical exfoliation.

CONCLUSION

In summary, we report a simple method for growing high optical quality monolayer MoS_2 directly on various insulating substrates, which should facilitate device fabrication without the need for a transfer process. The absence of impurity luminescence and the substantial room temperature polarization imply excellent crystal quality and the potential for optoelectronic applications without the need for low temperatures. The technique could also be applicable to other TMDCs.

METHODS

A MoS_2 powder source (Alfa Aesar, 99% purity) in an alumina boat is placed in the center of a horizontal quartz tube furnace (CARBOLITE 12/600 1200C tube furnace with 1 in. tube diameter), as illustrated in Figure 1. The insulating substrate (either 300 nm SiO_2/Si, (0001) sapphire, or normal glass) is cleaned in acetone, isopropyl alcohol, and deionized water and is placed downstream far from the oven center in a cooler zone (at ~650 °C during growth). The tube is initially pumped to a base pressure of 20 mTorr and flushed with the Ar carrier gas (~20 sccm) repeatedly at room temperature to remove oxygen contamination. With the carrier gas flowing and the pressure maintained at ~20 Torr, the furnace temperature is then increased to ~900 °C (~35 °C/min) and held there for 15−20 min before being allowed to cool naturally (see Supporting Information).

Conflict of Interest: The authors declare no competing financial interest.

Acknowledgment. This work was mainly supported by the U.S. Department of Energy, Office of Basic Energy Sciences, Division of Materials Sciences and Engineering (Awards DE-SC0008145 and DE-SC0002197). G.A. was supported by DARPA N66001-11-1-4124.

Supporting Information Available: Temperature profile of the growth, AFM characterization on the sapphire substrate, and complementary data for the PL polarization. This material is available free of charge *via* the Internet at http://pubs.acs.org.

REFERENCES AND NOTES

1. Novoselov, K. S.; Jiang, D.; Schedin, F.; Booth, T. J.; Khotkevich, V. V.; Morozov, S. V.; Geim, A. K. Two-Dimensional Atomic Crystals. *Proc. Natl. Acad. Sci. U.S.A.* **2005**, *102*, 10451–10453.
2. Coleman, J. N.; Lotya, M.; O'Neill, A.; Bergin, S. D.; King, P. J.; Khan, U.; Young, K.; Gaucher, A.; De, S.; Smith, R. J.; *et al.* Two-Dimensional Nanosheets Produced by Liquid Exfoliation of Layered Materials. *Science* **2011**, *331*, 568.
3. Mak, K. F.; Lee, C.; Hone, J.; Shan, J.; Heinz, T. F. Atomically Thin MoS_2: A New Direct-Gap Semiconductor. *Phys. Rev. Lett.* **2010**, *105*, 136805.
4. Splendiani, A.; Sun, L.; Zhang, Y.; Li, T.; Kim, J.; Chim, C.-Y.; Galli, G.; Wang, F. Emerging Photoluminescence in Monolayer MoS_2. *Nano Lett.* **2010**, *10*, 1271–1275.
5. Xiao, D.; Liu, G.-B.; Feng, W.; Xu, X.; Yao, W. Coupled Spin and Valley Physics in Monolayers of MoS_2 and Other Group-VI Dichalcogenides. *Phys. Rev. Lett.* **2012**, *108*, 196802.
6. Radisavljevic, B.; Radenovic, A.; Brivio, J.; Giacometti, V.; Kis, A. Single-Layer MoS_2 Transistors. *Nat. Nanotechnol.* **2011**, *6*, 147–150.
7. Ross, J. S.; Wu, S.; Yu, H.; Ghimire, N. J.; Jones, A. M.; Aivazian, G.; Yan, J.; Mandrus, D. G.; Xiao, D.; Yao, W.; *et al.* Electrical Control of Neutral and Charged Excitons in a Monolayer Semiconductor. *Nat. Commun.*, **2012**, DOI: arXiv:1211.0072.
8. Mak, K. F.; He, K.; Shan, J.; Heinz, T. F. Control of Valley Polarization in Monolayer MoS_2 by Optical Helicity. *Nat. Nanotechnol.* **2012**, *7*, 494–498.
9. Zeng, H.; Dai, J.; Yao, W.; Xiao, D.; Cui, X. Valley Polarization in MoS_2 Monolayers by Optical Pumping. *Nat. Nanotechnol.* **2012**, *7*, 490–493.
10. Cao, T.; Wang, G.; Han, W.; Ye, H.; Zhu, C.; Shi, J.; Niu, Q.; Tan, P.; Wang, E.; Liu, B.; *et al.* Valley-Selective Circular Dichroism of Monolayer Molybdenum Disulphide. *Nat. Commun.* **2012**, *3*, 887.
11. Xiao, D.; Yao, W.; Niu, Q. Valley-Contrasting Physics in Graphene: Magnetic Moment and Topological Transpor. *Phys. Rev. Lett.* **2007**, *99*, 236809.
12. Yao, W.; Xiao, D.; Niu, Q. Valley-Dependent Optoelectronics from Inversion Symmetry Breaking. *Phys. Rev. B* **2008**, *77*, 235406.
13. Wu, S.; Ross, J.; Aivazian, G.; Jones, A.; Fei, Z.; Liu, G.; Zhu, W.; Xiao, D.; Yao, W.; Cobden, D.; *et al.* Electrical Tuning of Valley Magnetic Moment *via* Symmetry Control. *Nat. Phys.* **2013**, DOI: 10.1038/nphys2524.
14. Radisavljevic, B.; Whitwick, M. B.; Kis, A. Integrated Circuits and Logic Operations Based on Single-Layer MoS_2. *ACS Nano* **2011**, *5*, 9934–9938.
15. Zhou, K. G.; Mao, N. N.; Wang, H. X.; Peng, Y.; Zhang, H. L. A Mixed-Solvent Strategy for Efficient Exfoliation of Inorganic Graphene Analogues. *Angew. Chem., Int. Ed.* **2011**, *50*, 10839–10842.
16. Eda, G.; Yamaguchi, H.; Voiry, D.; Fujita, T.; Chen, M.; Chhowalla, M. Photoluminescence from Chemically Exfoliated MoS_2. *Nano Lett.* **2011**, *11*, 5111–5116.
17. Peng, Y.; Meng, Z.; Zhong, C.; Lu, J.; Yu, W.; Jia, Y. B.; Qian, Y. Hydrothermal Synthesis and Characterization of Single-Molecular-Layer MoS_2 and $MoSe_2$. *Chem. Lett.* **2001**, *30*, 772–773.
18. Shi, Y.; Zhou, W.; Lu, A.-Y.; Fang, W.; Lee, Y.-H.; Hsu, A. L.; Kim, S. M.; Kim, K. K.; Yang, H. Y.; Li, L.-J.; *et al.* van der Waals Epitaxy of MoS_2 Layers Using Graphene as Growth Templates. *Nano Lett.* **2012**, *12*, 2784–2791.
19. Hadouda, H.; Pouzet, J.; Bernede, J. C.; Barreau, A. MoS_2 Thin Film Synthesis by Soft Sulfurization of a Molybdenum Layer. *Mater. Chem. Phys.* **1995**, *42*, 291–297.
20. Gutiérrez, H. R.; Perea-López, N.; Elías, A. L.; Berkdemir, A.; Wang, B.; Lv, R.; López-Urías, F.; Crespi, V. H.; Terrones, H.; Terrones, M. Extraordinary Room-Temperature Photoluminescence in Triangular WS_2 Monolayers. *Nano Lett.* **2012**, DOI: 10.1021/nl3026357.
21. Zhan, Y.; Liu, Z.; Najmaei, S.; Ajayan, P. M.; Lou, J. Large-Area Vapor-Phase Growth and Characterization of MoS_2 Atomic Layers on a SiO_2 Substrate. *Small* **2012**, *8*, 966–971.
22. Lee, Y.-H.; Zhang, X.-Q.; Zhang, W.; Chang, M.-T.; Lin, C.-T.; Chang, K.-D.; Yu, Y.-C.; Wang, J. T.-W.; Chang, C.-S.; Li, L.-J.; *et al.* Synthesis of Large-Area MoS_2 Atomic Layers with Chemical Vapor Deposition. *Adv. Mater.* **2012**, *24*, 2320–2325.
23. Sallen, G.; Bouet, L.; Marie, X.; Wang, G.; Zhu, C. R.; Han, W. P.; Lu, Y.; Tan, P. H.; Amand, T.; Liu, B. L.; *et al.* Robust Optical Emission Polarization in MoS_2 Monolayers through Selective Valley Excitation. *Phys. Rev. B* **2012**, *86*, 081301.
24. Kong, D.; Dang, W.; Cha, J. J.; Li, H.; Meister, S.; Peng, H.; Liu, Z.; Cui, Y. Few-Layer Nanoplates of Bi_2Se_3 and Bi_2Te_3 with Highly Tunable Chemical Potential. *Nano Lett.* **2010**, *10*, 2245–2250.
25. van der Zande, A. M.; Huang, P. Y.; Chenet, D. A.; Berkelbach, T. C.; You, Y.; Lee, G.-H.; Heinz, T. F.; Reichman, D. R.; Muller, D. A.; Hone, J. C. Grains and Grain Boundaries in Highly Crystalline Monolayer Molybdenum Disulfide. **2013**, DOI: arXiv:1301.1985 (arXiv preprint).
26. Najmaei, S.; Liu, Z.; Zhou, W.; Zou, X.; Shi, G.; Lei, S.; Yakobson, B.; Idrobo, J.-C.; Ajayan, P. M.; Lou, J. Vapor Phase Growth and Grain Boundary Structure of Molybdenum Disulfide Atomic Layers. **2013**, DOI: arXiv:1301.2812 (arXiv preprint).
27. Ni, Z. H.; Wang, H. M.; Kasim, J.; Fan, H. M.; Yu, T.; Wu, Y. H.; Feng, Y. P.; Shen, Z. X. Graphene Thickness Determination Using Reflection and Contrast Spectroscopy. *Nano Lett.* **2007**, *7*, 2758–2763.
28. Lee, C.; Yan, H.; Brus, L. E.; Heinz, T. F.; Hone, J.; Ryu, S. Anomalous Lattice Vibrations of Single- and Few-Layer MoS_2. *ACS Nano* **2010**, *4*, 2695–2700.
29. Jiménez Sandoval, S.; Yang, D.; Frindt, R. F.; Irwin, J. C. Raman Study and Lattice Dynamics of Single Molecular Layers of MoS_2. *Phys. Rev. B* **1991**, *44*, 3955–3962.
30. Korn, T.; Heydrich, S.; Hirmer, M.; Schmutzler, J.; Schuller, C. Low-Temperature Photocarrier Dynamics in Monolayer MoS_2. *Appl. Phys. Lett.* **2011**, *99*, 102109–102103.